CORA Cork Open Research Archive
Cartlann Taighde Oscailte Chorcaí

Title	Practical assessment of hardware limitations on power aware wireless sensor networks - An anti-windup approach
Author(s)	Walsh, Michael; Mahdi Alavi, Seyed Mohammad; Hayes, Martin J.
Publication date	2010
Original citation	Walsh, M. J., Mahdi Alavi, S. M., Hayes, M. J., 2010. Practical assessment of hardware limitations on power aware wireless sensor networks - An anti-windup approach. International Journal of Robust and Nonlinear Control, 20(2), pp.194-208
Type of publication	Article (peer-reviewed)
Link to publisher's version	http://dx.doi.org/10.1002/rnc.1475 Access to the full text of the published version may require a subscription.
Rights	© 2010 John Wiley & Sons, Ltd.
Item downloaded from	http://hdl.handle.net/10468/184

University College Cork, Ireland
Coláiste na hOllscoile Corcaigh

Practical assessment of hardware limitations on power aware Wireless Sensor Networks - an anti-windup approach[†]

M. J. Walsh[a*], S. M. Mahdi Alavi[b] and M. J. Hayes[c]

[a] *Clarity Center for Web Technologies, Tyndall National Institute Lee Maltings,*
University College Cork, Ireland.
[b] *School of Engineering Science, Simon Fraser University, British Columbia, Canada.*
[c] *Wireless Access Research Centre, Department of Electronic and Computer Engineering,*
University of Limerick, Ireland.

SUMMARY

This work considers the effect of hardware constraints that typically arise in practical "power-aware" wireless sensor network systems. A rigorous methodology is presented that quantifies the effect of output power limit and quantisation constraints on Bit Error Rate (BER) performance. The approach uses a novel, intuitively appealing means of addressing the output power constraint, wherein the attendant saturation block is mapped from the output of the plant to its input and compensation is then achieved using a robust Anti-Windup scheme. A priori levels of system performance are attained using a quantitative feedback theory approach on the initial, linear stage of the design paradigm. This hybrid design is assessed experimentally using a fully compliant 802.15.4 testbed where mobility is introduced through the use of autonomous robots. A benchmark comparison between the new approach and a number of existing strategies is also presented.

KEY WORDS: *Anti-Windup, Power Control, Wireless Sensor Network, Hybrid Control*

*Correspondence to: Tyndall National Institute, Lee Maltings, University College Cork, Cork, Ireland
`michael.walsh@tyndall.ie, mahdi.s.alavi@ul.ie, martin.j.hayes@ul.ie`

1. INTRODUCTION

Wireless sensor networks (WSNs) can be loosely defined as a linked list of (hopefully inexpensive) miniature devices that are capable of computation, communication and sensing. Originally conceived as a replacement for an equivalent wired communications network, the application space has extended at an exponential rate to encompass habitat, ecosystem, seismic and industrial process monitoring, security and surveillance, rapid emergency response and wellness maintenance [1, 2]. This paper considers that application subspace where battery life is a significant constraint. As it is commonly the case that up to 70% of the energy consumed by a WSN node is due to data transmission [3], it is natural to consider active power control in this context. However it is also invariably the case that only a finite number of transmission power levels will be supported by the device hardware at any instant. Coupling this fact with a requirement that some lower bound should exist on the information being transmitted - consider the case of vital biometric data that must continually be available to a health care provider for instance [4] - it is clear that this problem space poses an interesting challenge.

The goal of this work is to dynamically adjust device transmitter power, from a finite list of available levels, in a distributed manner so that the power consumption is minimized while also maintaining sufficient transmission quality. In this work the received signal strength indicator (RSSI) is selected as the dynamic variable to manage this objective. In the past it has been suggested that RSSI was a less than ideal metric for control. This claim however was based on experimentation with early platforms that used radios, e.g. the Texas Instruments CC1000, where hardware miscalibration or drift was often a problem. However in recent times the use of RSSI has undergone something of a renaissance, with newer radios such as the 802.15.4 compliant TI CC2420 exhibiting highly stable performance. For example in [5], RSSI was seen

to exhibit quite insignificant time-variability as long as it stayed above an a priori defined threshold level. Other work [3] has also established a good relationship between RSSI and signal to noise plus interference ratio (SINR). This relationship is exploited here to achieve pre-specified performance objectives in terms of packet error rate (PER).

1.1. Problem formulation

This work concentrates on assessing the effect that the limited power transmission capabilities of a typical mobile node within a practical sensor network will have on performance. These natural hardware constraints will impose saturation type limits that will obviously severely degrade network performance. A literature already exists regarding the treatment of these constraints. For instance, in [6] and [7] distributed power control schemes have been described wherein the minimum carrier to interference ratio (CIR) is maximised subject to a constraint on the maximum power. Other more recent advances in control design theory that explicitly deal with output constraints have also been reported [8]. While these methods have had some success in dealing with output saturation constraints, there also exists a vast, more extensive literature treating linear systems that are subject to input saturation constraints [9]. It is therefore intuitively appealing to consider the virtual mapping of the output saturation constraint for the problem at hand to the input of the plant or the output of a suitable controller. Using this approach allows for a more conservative controller design approach that will facilitate graceful performance degradation in the face of nonlinearity.

This work introduces a two step AW design procedure for this problem. The first step is to design a linear controller, ignoring the inherent nonlinear constraints that are placed on the system, that uses a Quantitative Feedback Theory (QFT) approach to provide both robust

stability and nominal performance in the linear region of operation. A feature of this first step is that it naturally bounds the time domain response of the system for a particular power level and provides a basis for assessing how a change in the quantisation noise caused by power level selection will affect performance. The second step in the procedure incorporates recent advances in AW theory to minimize performance degradation in the face of actuator constraints. The technique employed here is commonly described as the Weston-Postlethwaite Anti-Windup (WP-AW) Synthesis. First presented in [10] and later in its discretized form in [11], this technique uses an $\mathcal{L}_2$ approach in conjunction with linear matrix inequality (LMI) optimization techniques to ensure that, during saturation, system performance remains as close to nominal linear operation as possible and furthermore returns to the linear operating region as quickly as possible.

In this work the analysis machinery is shown to be capable of quantifying the effect of quantisation noise in the WSN node on closed loop system performance, (In this context on packet Bit Error Rate BER). For any transceiver a discrete number of transmission power levels are available and switching between these power levels necessarily introduces a quantisation noise that will adversely affect the gain and phase margin properties of a design. The effect of this quantisation noise is represented by upper and lower bounds on the complementary sensitivity function $T_U(Z)$ and $T_L(Z)$ respectively in this work. The approach adopted in this regard is similar to that suggested in [12] where the plant model for the WSN device is no longer represented by an integrator. However rather than replace the plant model with a direct feedthrough term, (i.e., for a device G and power command update p_i the plant output is $G(p_i) = p_i$), the plant is herein modelled as a low pass filter possessed of sufficient available bandwidth to be robust to a particular level of quantisation noise.

This paper is organized as follows. Section 2 introduces some nomenclature and defines the network model that has been adopted throughout the work. In section 3 the linear controller design procedure is outlined, followed by the AW controller design stage in section 4. Section 5 firstly presents a practical assessment of performance with and without AW for the testbed under consideration and secondly provides a benchmark comparison between the new approach and some more traditional power control schemes. Some concluding remarks and some related future research themes are also provided.

2. THE WIRELESS CHANNEL MODEL

A description of the wireless channel model is now provided. Note that a value in the linear scale is represented by $\bar{g}$ and g is it's corresponding value in dB namely $g = 10log_{10}\bar{g}$.

2.1. The saturation function

The saturation function is defined as

$$sat(u) := [sat_1(u_1), ..., sat_m(u_m)], \tag{1}$$

where $sat_i(u_i) := sign(U_i) \times min\{|u_i|, \tilde{u}_i\}$, with $\tilde{u}_i > 0$ is the ith saturation limit. Note the $sat(.)$ function in (1), belongs to sector $[0, 1]$ and is assumed locally Lipschitz. The following set is defined

$$\mathcal{U} := [-\tilde{u}_1, \tilde{u}_1] \times, ..., \times [-\tilde{u}_m, \tilde{u}_m], \tag{2}$$

where clearly $sat(u) = u$, $\forall u \in \mathcal{U}$. This is the set in which the saturation behaves linearly which in turn will imply that nominal closed loop system conditions are exhibited.

2.2. System Model

The system is illustrated in figure 1(a). Information feedback is adopted throughout so that the system output $y(k)$ (RSSI) can be assumed to be fully measurable at the receiver. Other signals include controller output $u(k)$ (power level), reference input $r(k)$ (reference RSSI) and quantisation noise $q(k)$ associated with switching between the discrete transceiver power levels. $d(k)$ is a disturbance to the system and comprises of channel attenuation, interference, measurement error and thermal noise. The plant $G(z)$ is represented by $G(z) = [G_1(z)\ G_2(z)]$, where $G_1(z)$ and $G_2(z)$ are the disturbance feedforward and feedback parts of $G(z)$ respectively. Given that no disturbance model is available in the form of a transfer function, $G_1(z)$ is taken to be $G_1 = I$ where I is the identity matrix. The controller $K(z)$ takes the form $K(z) = [K_1(z)\ K_2(z)]$ a standard two degree of freedom structure. Figure 1(b) illustrates the system where the saturation block has been mapped from the output of the system to the input. Note how $u_m(k)$ is now the saturated input to the plant. In order to represent this mapped saturation function the set

$$\mathcal{U}_n := [-\tilde{u}_1/h_{G_2}, \tilde{u}_1/h_{G_2}]\times, ..., \times[-\tilde{u}_m/h_{G_2}, \tilde{u}_m/h_{G_2}], \tag{3}$$

is defined where h_{G_2} is the gain of the transfer function G_2, selected as a low pass filter with sufficient bandwidth to eliminate quantisation noise. $G_2(z)$ is represented by

$$G_2(z) = \frac{1}{1.1z - 0.9}. \tag{4}$$

As mentioned previously a similar approach to [3] is used to directly estimate the SINR using the RSSI. This facilitates the selection of a setpoint or reference RSSI value that relates directly
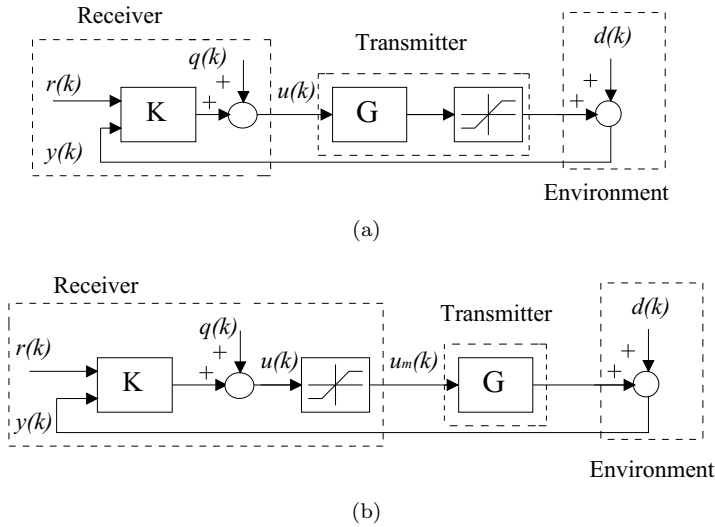
(a)

(b)

Figure 1. Wireless System Model with (a) Saturation block at the output, (b) Saturation block mapped from output to input.

to PER. Given the analysis machinery proposed in this work is practically implemented on an 802.15.4 compliant testbed it is worthwhile using the 802.15.4 standard as an example. To expand the 802.15.4 standard [13] defines bit error rate (BER) when operating at a frequency of 2.4GHz as

$$BER = \frac{8}{15} \times \frac{1}{16} \times \sum_{k=2}^{16} -1^k \left(\begin{array}{c} 16 \\ k \end{array} \right) e^{20 \times SINR \times (\frac{1}{k} - 1)}, \tag{5}$$

The PER can then be obtained from

$$PER = 1 - (1 - BER)^{PL} \tag{6}$$

where PL is packet length including the header and payload. Establishing a relationship between RSSI and SINR and subsequently PER can therefore help to pre-specify levels of

system performance. For a sensor node i, the SINR is given by, [3]

$$\gamma_i(k) = RSSI(k) - C - 30 \tag{7}$$

where the addition of the scalar term 30 accounts for the conversion from dBm to dB and C is the measurement offset.

The SINR of the i-th node for a network consisting of n nodes communicating with a receiver is given by:

$$\bar{\gamma}_i(k) \triangleq \frac{\bar{p}_i(k)\bar{g}_i(k)}{\sum\limits_{j \in \mathcal{Z}, i \neq j} \bar{p}_j(k)\bar{g}_j(k) + \bar{n}_i(k)} \triangleq \frac{\bar{p}_i(k)\bar{g}_i(k)}{\bar{I}_i} \tag{8}$$

where $\bar{g}_i(k)$ is a time-varying multiplicative power gain between the i-th node and the receiver. $\bar{g}_i$ is affected by a number of factors including path loss, shadowing, multipath fading and autocorrelation, a detailed treatment for each phenomenon is given in [14]. $\bar{I}_i = \sum\limits_{j \in \mathcal{Z}, i \neq j} \bar{p}_j(k)\bar{g}_j(k) + \bar{n}_i(k)$ comprises of interference and $\bar{n}_i$, the power of the white noise at the receiver. $\mathcal{Z}$ is the set of all nodes interfering with node i. Representing 8 in dB results in:

$$\gamma_i(k) = p_i(k) + g_i(k) - I_i(k) \tag{9}$$

Subseqeuntly taking (7) and substituting for $\gamma_i(k)$ in (9) results in

$$p_i(k) + g_i(k) - I_i(k) = RSSI(k) - C - 30 \tag{10}$$

which is equivalent to

$$RSSI(k) = p_i(k) + d(k) \tag{11}$$

where $d(k) = g_i(k) - I_i(k) + C + 30$. The disturbance to the system $d(k)$ from figure 1(b)

therefore comprises of channel attenuation, interference, measurement error and thermal noise.

3. ROBUST POWER TRACKING CONTROLLER DESIGN

The first step in the controller design procedure requires a linear controller design stage that ignores the control input nonlinearity. The approach adopted here is based on quantitative feedback theory (QFT) and addresses both robust stability and performance. QFT design was first developed by Horowitz and is essentially a Two-Degree-of-Freedom (2DOF) frequency domain technique, as illustrated in figure 2. The scheme achieves client-specified levels of desired performance over a region of parametric plant uncertainty, determined *a priori* by the engineer, [15]. The methodology requires that the desired time-domain responses are translated into frequency domain tolerances, which in turn lead to design bounds in the loop function on the Nichols chart. In a QFT design, the responsibility of the feedback compensator, $K_2(z)$, is to focus primarily on attenuating the undesirable effects of uncertainty, disturbance and noise. Having arrived at an appropriate $K_2(z)$, a pre-filter $K_1(z)$, is then designed so as to shift the closed-loop response to the desired tracking region specified *a priori* by the engineer. The approach requires that the designer select a set of desired specifications in relation to the magnitude of the frequency response of the closed-loop system, thereby achieving robust stability *and* performance.
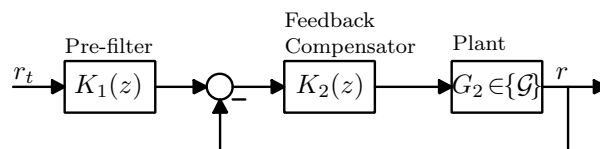

Figure 2. 2DOF feedback system based on quantitative feedback theory.

3.1. Determination of specifications for the Quantisation Noise Problem

In a QFT paradigm, the notion of robust stability is usually incorporated into gain and phase margins through the use of the following constraint:

$$\left| \frac{K_2 G_2}{1 + K_2 G_2}(z) \right|_{z=e^{j\omega T_s}} \leq \mu, \tag{12}$$

$$for \ all \ G_2 \in \{\mathcal{G}\}, \omega \in [0, \pi/T_s].$$

This subsection considers how quantisation noise can be represented using this methodology. For a particular sampling frequency, (chosen as $T_s = 3(sec)$ in this case), a (nominal) plant is given by 4, as discussed in section 2. This stability criterion corresponds to lower bounds on the gain margin of $K_M = 1 + 1/\mu$ and the phase margin angle of $\phi_M = 180° - \cos^{-1}(0.5/\mu^2 - 1)$, [16]. Throughout the design $\mu = 1.5$ is adopted, thereby guaranteeing a phase and gain margin equal to $50°$ and 1.44, respectively. The introduction of quantisation noise will necessarily reduce both these margins. The following design constraint can be used to ensure adequate tracking performance,

$$|T_L(j\omega)| \leq \left| \frac{K_2 G_2}{1 + K_2 G_2}(z) \right|_{z=e^{j\omega T_s}} \leq |T_U(j\omega)|, \tag{13}$$

$$for \ all \ G_2 \in \{\mathcal{G}\}, \omega \in [0, \omega_h].$$

where $T_L(j\omega)$ represents desired (overdamped) performance without quantisation noise and $T_U(j\omega)$ represents system response (underdamped) with the noise included. ω_h denotes desired performance bandwidth. It should be noted that the effect of reducing the available number of power levels in this setting will correspond to a *reduction* in the gap between $T_L(j\omega)$ and $T_U(j\omega)$. Equation (13) implies that the system RSSI will be adequate if it is possible to design

a filter that can place the system loop gain response within the pre-defined region specified by upper and lower bounds $T_U(z)$ and $T_L(z)$, respectively. Consider the following example. Suppose a particular level of performance is required so that *i)* the RSSI should be required to settle around the target value of $5 \leq t_{ss} \leq 25(s)$, and *ii)* damping factor $\xi = 0.5$, is desired to reduce outage probability at the outset of communication, the following transfer functions can be selected so as to achieve the desired tracking bounds when there exist 31 possible transceiver power levels:

$$T_U(z) = \frac{0.9945z + 0.3891}{z^2 + 0.2928z + 0.09072} \tag{14}$$

$$T_L(z) = \frac{0.1219z + 0.08167}{z^2 - 1.098z + 0.3012} \tag{15}$$

A reduction in the number of available power levels will result in a reduction in the gap between $T_L(Z)$ and $T_U(Z)$. In order to provide robustness link uncertainties and multiple user interference are treated as disturbances. Here, it is sufficient to over-bound the transfer function from $\overline{D}_i(k)$ to $\overline{r}_i(k)$ with an appropriate disturbance rejection ratio as follows:

$$\left| \frac{1}{1 + K_2 G_2}(z) \right| \leq |W_D(z)|, \tag{16}$$

$$z = e^{j\omega T_s} \text{ for all } G_2 \in \{\mathcal{G}\}, \omega \in [0, \omega_h].$$

where W_D represents a weighting function on the required levels of disturbance rejection. There must always be a trade off between stability and disturbance attenuation that has to be taken into consideration in the selection of W_D. Sweeping W_D from 0.1 to 1 demonstrates that $W_D = 0.9$ provides a reasonable disturbance attenuation ratio and produces a feasible controller that appropriately makes the trade-off. Based on the desired tracking upper and
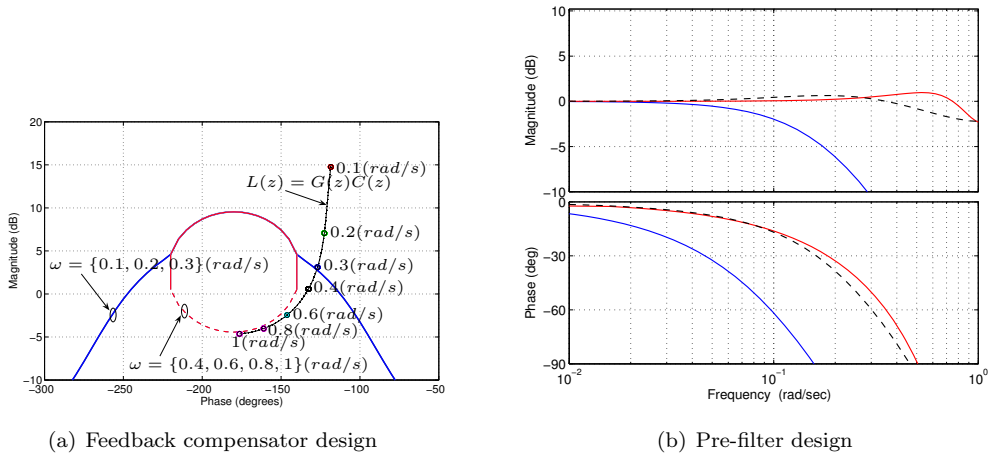
PSfrag replacements

(a) Feedback compensator design

(b) Pre-filter design

Figure 3. QFT controllers. All design bounds are satisfied by $C(z)$, and $F(z)$.

lower bounds, performance bandwidth is selected as $\omega_h = 0.3(rad/s)$.

3.2. Feedback compensator design

Using the MATLAB QFT-Toolbox [16], The design bounds associated with equation (12) and (16) are computed for $\{0.05, 0.1, 0.2, 0.3, 0.4, 0.5, 0.6, 0.7, 0.8, 0.9, 1\}$ (rad/s), and $\{0.05, 0.1, 0.2, 0.3\}$ (rad/s) respectively. The intersection of the bounds at each design frequency is the final bound taken for the design of the feedback compensator, $K_2(z)$. Figure 3(a) shows the obtained QFT design bounds. $K_2(z)$ is designed by adding appropriate poles and zeros to the loop function so that the nominal loop function frequency response satisfies the worst case design specification for the bounds at each frequency. For robustness, the nominal loop function must be shaped such that the frequency response lies above the design bounds at each design frequency and does not enter the U-contours described in figure 3(a). Moreover the critical point $(-180°, 0dB)$ must also be avoided. Figure 3(a), illustrates that (17) satisfies

the design bounds:

$$K_2(z) = \frac{z - 0.6622}{0.7103z - 0.7103} \qquad (17)$$

Remarks

a) Figure 3(a) implies that similar disturbance attenuation bounds will obtain for different design frequencies in this case study. An analagous result is also valid for robust stability bounds. In this case it is required that the worst case, which is related to a frequency range close to the performance bandwidth, be satisfied. It should be noted however that the higher the performance bandwidth, the larger the controller gain that is required. Therefore, there will be always a tradeoff in the design.

b) Given that a deterministic low-pass filter has been used as the plant in this case study, the Matlab QFT-toolbox is not able to generate tracking design bounds in Nichols chart.

3.3. Pre-filter design

The closed-loop transfer function is shaped using $K_1(z)$ to place the system frequency response between two pre-defined lower and upper bounds, [15], [16]. Figure 3(b) shows that by using the following pre-filter, the closed-loop transfer function will place between $T_L(z)$ and $T_U(z)$. (18) satisfies the design bounds:

$$K_1(z) = \frac{1.4127z}{z - 0.4127} \qquad (18)$$

4. WESTON-POSTLETHWAITE ANTI-WINDUP (WP-AW) SYNTHESIS

In state space format the wireless network model introduced in section 2 can be represented by

$$G(z) \sim \begin{cases} x_p(k+1) = A_p x_p(k) + B_p u_m(k) + B_{pd} d(k) \\ \\ y(k) = C_p x_p(k) + D_p u_m(k) + D_{pd} d(k) \end{cases} \tag{19}$$

where the signals are labelled as in section 2. The disturbance feedforward and feedback parts of $G(z)$ can be described by

$$G_1(z) = \left[\begin{array}{c|c} A_p & B_{pd} \\ \hline C_p & D_{pd} \end{array} \right] \quad , \ G_2(z) = \left[\begin{array}{c|c} A_p & B_p \\ \hline C_p & D_p \end{array} \right] \tag{20}$$

Consider the generic AW configuration shown in figure 4. As illustrated above the plant takes the form $G = [G_1 \ G_2]$, the linear controller is represented by $K = [K_1 \ K_2]$, and $\Theta = [\theta_1 \ \theta_2]$ is the AW controller becoming active only when saturation occurs. Given the difficulty in analyzing the stability and performance of this system we now adopt a framework first introduced in [10] for the problem at hand. This approach reduces to a linear time invariant Anti-Windup scheme that is optimized in terms of one transfer function $M(z)$ shown in figure 5. It was shown in [10] that the performance degradation experienced by the system during saturation is directly related to the mapping $\mathcal{T} : u_{lin} \rightarrow y_d$. This may not be clear at first glance, however if one looks at the equivalent representation of the system illustrated in figure 6 and derived in [10], it can be seen that the decoupled system is divided into three sections: the nominal linear system, the disturbance filter and the nonlinear loop. Note that from figure 6 $M - I$ is considered for stability of $\mathcal{T}$ and $G_2 M$ determines the systems recovery after
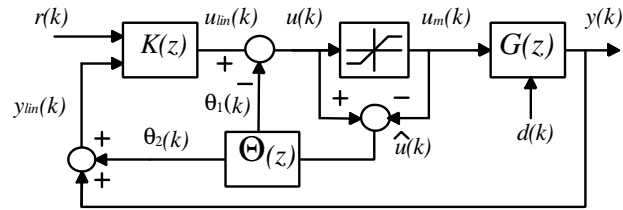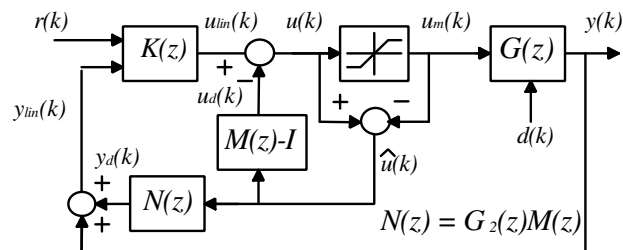
Figure 4. A generic anti-windup scenario.

Figure 5. Weston Postlethwaite Anti-Windup conditioning technique.

saturation. This decoupled representation vividly illustrates how this mapping can be utilized as a performance measure for the AW controller. To quantify this an AW controller is selected such that the l_2-gain, $\|\mathcal{T}\|_{i,2}$, of the operator $\mathcal{T}$

$$\|\mathcal{T}\|_{i,2} = \sup_{0 \neq u_{lin} \in \mathcal{L}_2} \frac{\|y_d\|_2}{\|u_{lin}\|_2}$$

where the l_2 norm $\|x\|_2$ of a discrete signal $x(h), (h = 0, 1, 2, 3, ...)$ is

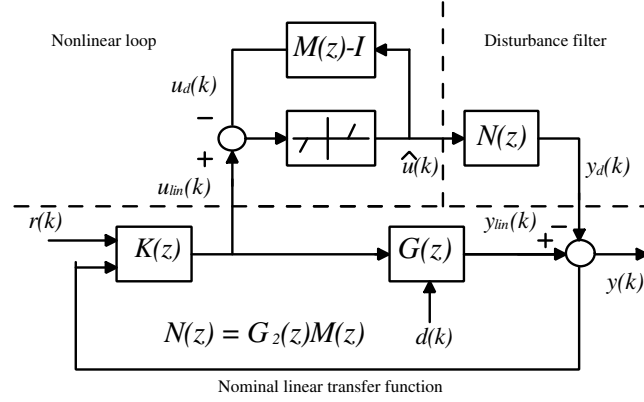$$\|x\|_2 = \sqrt{\sum_{h=0}^{\infty} \|x(h)\|^2}$$

Figure 6. Equivalent representation WPAW conditioning technique.

4.1. Static anti-windup synthesis

Static AW has an advantage in that it can be implemented at a much lower computational cost and adds no additional states to the closed loop system. Full order AW synthesis or AW with order equal to the plant will often lead to less response deterioration during saturation, however significant computation is required. This is often unacceptable, especially in systems that are of higher order and where additional states are undesirable. For this reason it is common practice that most windup problems are suppressed using static compensators, see for example [17]. Using the aforementioned conditioning technique via $M(z)$, outlined in [18], Θ from figure 4 is given by

$$\begin{bmatrix} \theta_1 \\ \theta_2 \end{bmatrix} = \Theta \hat{u} = \begin{bmatrix} \theta_1 \\ \theta_2 \end{bmatrix} \hat{u}$$

where u is derived from figure 4 and figure 5 respectively, as

$$u = K_1 r + K_2 y - [(I - K_2 G_2)M - I]\hat{u}$$

$$u = K_1 r + K_2 y + (K_2 \Theta_2 - \Theta_1)\hat{u}$$

Thus $M(z)$ can be written as

$$M = (I - K_2 G_2)^{-1}(-K_2 \Theta_2 + \Theta_1 + I)$$

The goal of the static AW approach is therefore to ensure that extra modes do not appear in the system. Since this will inevitably be the case it must be ensured that minimal realizations of the controller and plant are used [11]. A state space realization can then be formed

$$
\begin{bmatrix} M(z) - I \\ N(z) \end{bmatrix} \sim \begin{bmatrix} \dot{\bar{x}} \\ u_d \\ y_d \end{bmatrix} = \left[\begin{array}{c|c} \bar{A} & B_0 + \bar{B}\Theta \\ \hline \bar{C}_1 & D_{01} + \bar{D}_1\Theta \\ \bar{C}_2 & D_{02} + \bar{D}_2\Theta \end{array} \right] \begin{bmatrix} \bar{x} \\ \hat{u} \end{bmatrix}
\tag{21}
$$

where $\Theta = [\Theta_1' \Theta_2']'$ is a static matrix and $\bar{x}$, $\bar{A}$, B_0, $\bar{B}$, $\bar{C}_1$, D_{01}, $\bar{D}_1$, $\bar{C}_2$, D_{02} and $\bar{D}_2$ are minimal realizations given in appendix A.

In a similar manner to [19] a solution is obtained for the LMI in 22 with $Q > 0$, $U = diag(v_1, ... v_c) > 0$, $L \in \Re^{(c+n) \times n}$ (where $c = n$), and the minimized l_2 gain $\|\mathcal{T}\|_{i,2} < \gamma$ (where γ is the l_2 gain bound on $\mathcal{T}$). In this instance Θ is given by $\Theta = LQ^{-1}$ using which the controller in 21 can be synthesized.

$$
\begin{bmatrix}
-Q & -Q\bar{C}_1' & Q\bar{A}' & 0 & Q\bar{C}_2' \\
- & -X & UB_0 + L'\bar{B}' & I & UD_{02}' + L'\bar{D}_2' \\
- & - & -Q & 0 & 0 \\
- & - & - & -\gamma I & 0 \\
- & - & - & - & -\gamma I
\end{bmatrix} < 0
\tag{22}
$$

Where $X = 2U + D_{01}U + \bar{D}_1 L + U D'_{01} + L' \bar{D}'_1$. Such an $\mathcal{L}_2$ design for example [20] ensures that during saturation closed loop performance is achieved by staying close to the nominal design while the time spent in saturation is also jointly minimized. Applying this synthesis routine to our plant given by (4) and linear controller (17), the resultant controller is $\Theta = [-0.2049\ 0.6377]'$ obtained using the LMI toolbox in Matlab[†].

5. PRACTICAL IMPLEMENTATION: 802.15.4 WSN CASE STUDY

In this section the proposed hybrid design is assessed experimentally using a fully compliant 802.15.4 testbed. The effect that quantisation noise and output power saturation have on the system are examined and the means by which these effects are assessed is discussed. The analysis of the proposed controller is divided into two subsections. Firstly, the performance of the system with and without AW is examined to assess the benefits of AW. This subsection also contains an analysis of system performance with and without the pre-filter that is included as part of the linear design. Latterly, a benchmark comparison between the proposed methodology and other approaches traditionally used in wireless cellular networks is presented.

5.1. 802.15.4 Testbed Description

The experimental setup mimics a typical search and rescue type scenario and is shown in figure 7. It consists of six Tmote^{TM} nodes one of which acts as a base station. The Tmote Sky sensor node provides an embedded platform that incorporates a fully 802.15.4 compliant CC2420 transceiver using the Direct Sequence Spread Spectrum (DSSS) technique to code the

---

[†]The Mathworks Inc.

required data. Carrier Sensing Multiple Access/Collision Avoidance (CSMA/CA) is used to transmit the coded packets, preventing simultaneous communication between any two nodes and the base station which could result in packet collision and subsequent lost of data. It should be noted that such a stringent access technique can potentially result in under utilization of channel capacity. It will be a focus of future work to investigate the dynamic management of the carrier sense threshold so as to ensure optimal spatial reuse.

An RSSI measurement is provided in dBm by averaging the received signal power over 8 symbol periods or $128\mu s$. An interface between Matlab and TinyOS has been established using TinyOS Matlab tools written in Java. Sensor data packets are framed in 802.15.4 format and transmitted using the TinyOS library function Oscope. The base station bridges packets over the USB/Serial connection to a personal computer. The Matlab application identifies the

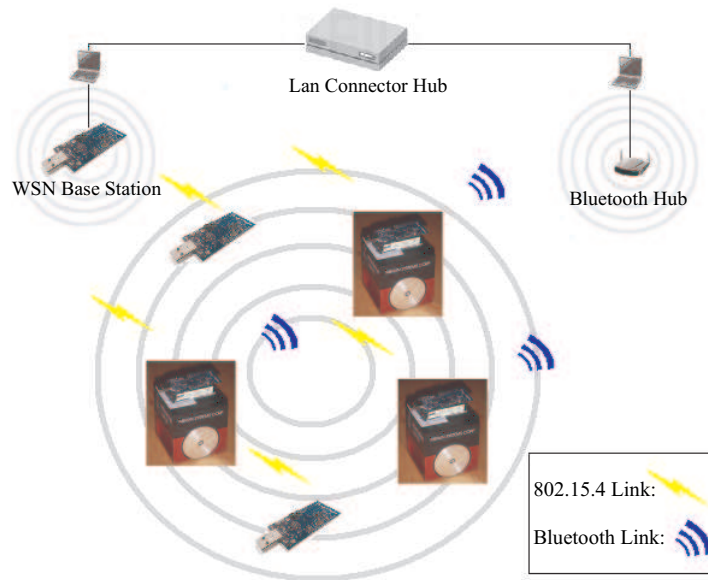Figure 7. 802.15.4 Wireless experimental scenario.

Figure 8. Dataflow in the network.

connection by its phoenixSource name e.g. 'network@localhost:9000' or by its serial port name

e.g. 'serial@COM3:tmote' and imports the packets directly into the Matlab environment. In

this scenario a Tmote can supply environmental information such as temperature, humidity

and ambient light level using onboard sensors. No new point of principle arises, from a power

control perspective, in the extension of the testbed to include safety critical sensor data. For

example the same communications module has also been used, (see [4] and references therein),

where the onboard 10-pin expansion port has provided an interface for an additional hardware

module to gather and process biometric data like e.g. ECG or blood oxygen levels.

Three of the Tmotes have been piggybacked onto fully autonomous MIABOT Pro miniature

mobile robots [21]. Each robot is controlled by an Atmel ATMega64 microcontroller which

runs at a speed of 14.5MIPS and is equipped with a 64kb flash. The ATMega64 is manually

programmed using the GNU Collection 'C' compiler. Commands are transferred to each robot

via a Bluetooth hub. Dataflow in the system is shown in figure 8.

5.2. Scenario Description and Performance Criteria

Each of the control strategies to be examined is tested using the setup of figure 7. Initially all five nodes are stationary and the experiment is executed five times using five randomly selected node positions. The experiment is 200(sec) in duration. One mobile node is then introduced to the system and the scenario is repeated again for 5 randomly chosen positions for the remaining 4 stationary nodes. A second and finally a third mobile is introduced and the scenario is repeated. Each approach is therefore evaluated for a total of 20 experiments, with each spending over an hour in operation with varied levels of mobility within the system. For consistency the trajectories along which the mobile robots move remain the same for each experiment.

A sampling frequency of $T_s = 3(sec)$ is used throughout and a target RSSI value of -55dBm is selected for tracking guaranteeing a PER of $< 1\%$, verified using equations 5, 6 and 7. The standard deviation of the RSSI tracking error is chosen as a performance criterion:

$$\sigma_e = \Big\{ \frac{1}{S} \sum_{k=1}^{S} [r(k) - RSSI(k)]^2 \Big\}^{\frac{1}{2}} \tag{23}$$

where S is the total number of samples and k is the index of these samples. Outage probability is defined as

$$P_o(\%) = \frac{the\ number\ of\ times\ that\ RSSI\ <\ RSSI_{th}}{the\ total\ number\ of\ iterations} \times 100 \tag{24}$$

where $RSSI_{th}$ is selected to be -57dBm, a value below which performance is deemed unacceptable in terms of PER. This can be easily verified again using equations 5, 6 and

7. To fully access each paradigm, some measure of power efficiency is also useful and here we define average power consumption as the average power consumed by all motes operating using a particular power control algorithm for the duration of an experiment. Therefore given that there are five motes in the cell power consumption is computed by first averaging the power consumed throughout the experiment on an individual basis and then the average of these five values yields an overall average result.

5.3. Justification and Improvements afforded by Anti-Windup

To justify the need for Anti-Windup, a number of experiments were conducted using the repeatable scenario outlined above. Firstly in order to motivate the need for the standard deviation performance criterion (23), the results for a single experiment are shown in figure 9(a). This experiment consists of one mobile node and uses the QFT controller design without AW but does incorporate a pre-filter. It can be observed that, without AW, the controller output when saturated begins to increase or 'wind-up' and as a result the system upon re-entry to the linear region of operation requires a substantial period of time to 'unwind'. This leads to dramatic performance degradation in terms of standard deviation from the setpoint. Figure 9(b) displays the results of the same experiment with AW in place. It is clear that while saturation cannot be avoided the 'wind-up' exhibited previously without AW is no longer present. Figure 10 gives a better idea of overall system performance. It is first worth noting the system performance with and without the pre-filter designed in section 3. Clearly the system with the pre-filter exhibits an improved standard deviation and outage probability. However, this improvement is accompanied by an attendant increase in power consumption as a result of a slightly more aggressive transient response, required to improve tracking. As our
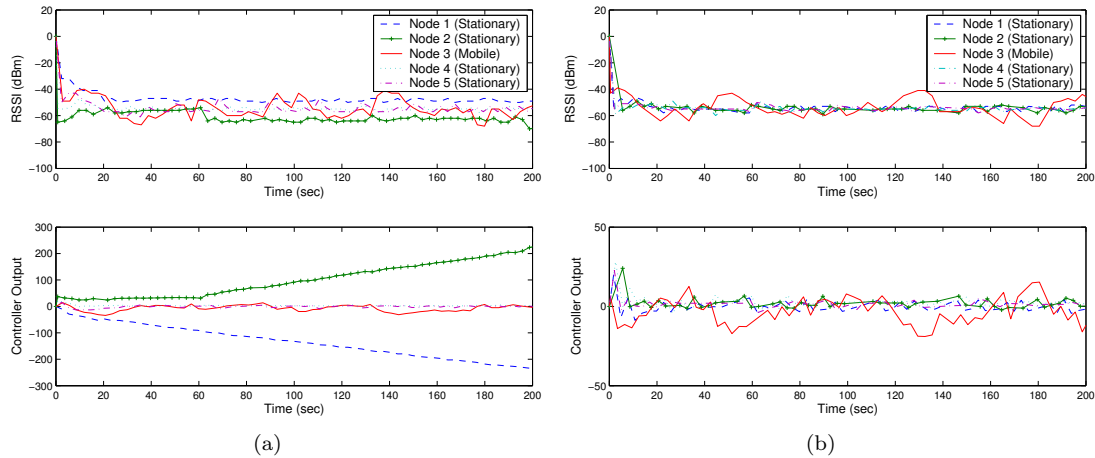
Figure 9. System response (a) without WPAW, (b) with WPAW.

Figure 10. Comparison with and without pre-filter and with and without AW.
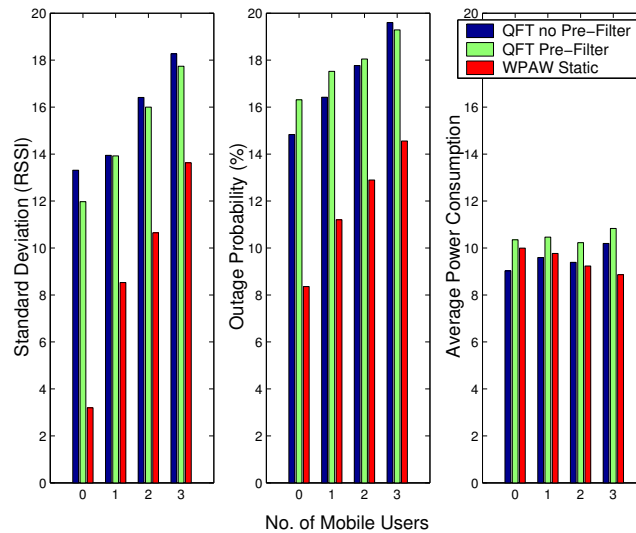
goal is to provide both robust stability (disturbance rejection) and performance (tracking), it is natural that the QFT design with pre-filter should be selected as the linear part of the hybrid design. The performance of the hybrid system is summarised in table 1, i.e. the system that incorporates QFT with a pre-filter and static AW, exhibits improvements in

Table I. CHARACTERISTICS: σ_e - Standard Deviation, P_o - Outage Probability, P_{av} - Average Power Consumption

No. of Mobiles	Adaptive			Conventional/ LMI			Hybrid QFT/ Static AW		
	σ_e	P_o	P_{av}	σ_e	P_o	P_{av}	σ_e	P_o	P_{av}
0	96	22.7	20.9	7.2	10.6	8.6	3.1	8.3	9.9
1	113	27.6	22.2	10.4	13.4	9	8.5	11.2	9.7
2	130.4	29.4	21.1	12.1	14.8	8.9	10.6	12.8	9.2
3	134.9	30.7	21.9	13.7	16.2	9.3	13.6	14.5	8.8

standard deviation, outage probability and power consumption. This highlights the benefits of considering system nonlinearities using an AW approach.

5.4. Effects of Quantisation Noise

To determine the effect of switching between the limited number of power levels that are available to the transceiver consider the performance specification bounds corresponding to equations 14 and 15, outlined in section 3. The analysis methodology can also be most useful in providing an assessment of the effect on performance that a switch in the number of active power levels within a transceiver will have. The performance specification explicitly considers the quantisation noise that must be tolerated and the design subsequently seeks to provide sufficient bandwidth to accommodate this noise.

5.5. Benchmark Comparative Study

In this section the performance of the WPAW Static controller is compared with fixed step, H∞/LMI and adaptive step active power control methods. A brief description of these alternative methods is now presented:

5.5.1. Fixed Step (Conventional) Size Power Control This method uses the scenario illustrated by 1(a) and is widely used in CDMA IS-95 systems due to its rapid convergence [14]. This strategy also assumes that G in 1(a) is an integrator, therefore the approach is implemented using the following power control law

$$y(k) = y(k-1) + \delta(r(k) - RSSI(k)) \tag{25}$$

where $y(k)$ is the transmission power and δ is the fixed step size (1 for the purposes of this experiment).

5.5.2. H∞/LMI Power Control This approach introduced in [22] solves the following H∞ tracking problem

$$\frac{\frac{1}{k_f} \sum_{k=0}^{k_f} e'(k) R_1 e(k)}{\frac{1}{k_f} \sum_{k=0}^{k_f} d'(k) R_2 d(k)} < \gamma^2 \tag{26}$$

where R_1 and R_2 are positive weighting factors for the designer and k_f is the total transmission data length. Given the relative low order of our distributed system this approach will yield the controller $K = 1$ which is equivalent to the conventional approach with step size equal to one. These two methods are therefore analyzed as one.

5.5.3. Adaptive Step Size Power Control This method uses the same power control law as the fixed step approach [14], however the parameter δ is updated depending on system requirements according to the following

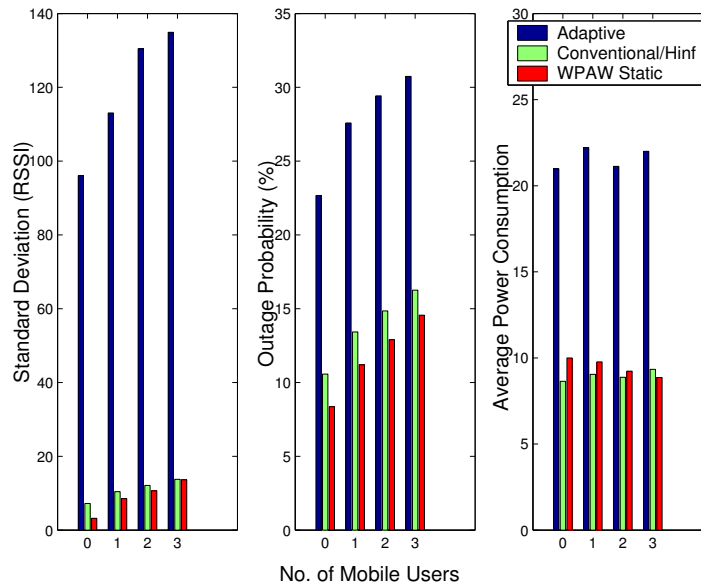$$\delta(k) = [\alpha \delta^2(k-1) + (1-\alpha)\sigma_e^2]^{\frac{1}{2}} \tag{27}$$

Figure 11. Comparison between adaptive, conventional/H∞ and WPAW Static approaches.

where as before σ_e is the sampled standard deviation of the power control tracking error and α is the forgetting factor, (assumed to be 0.95 here), introduced to smooth the measured RSSI signal which may be corrupted by noise.

Figure 11 and table 2 illustrate how the proposed hybrid system performs when compared to the approaches outlined above. Clearly the hybrid design outperforms the adaptive approach for all of the criterion and shows substantial improvement over the conventional/H∞ in terms of standard deviation and outage probability with low mobility in the system. However with fewer mobile nodes in the system the conventional/H∞ approach consumes less power. This is due to the aggressive action of the pre-filter that results in improved tracking performance. As the number of mobile users is increased the standard deviations of the hybrid design and the conventional/H∞ converge, however the hybrid design continues to exhibit improved outage probability. The average power consumption for the three approaches also converges,

Table II. CHARACTERISTICS: σ_e - Standard Deviation, P_o - Outage Probability, P_{av} - Average Power Consumption

No. of Mobiles	QFT without Pre-Filter			QFT with Pre-Filter			Hybrid QFT/ Static AW		
	σ_e	P_o	P_{av}	σ_e	P_o	P_{av}	σ_e	P_o	P_{av}
0	13.3	14.8	9	12	16.3	10.4	3.1	8.3	9.9
1	13.9	16.4	9.6	14	17.5	10.5	8.5	11.2	9.7
2	16.4	17.8	9.4	16	18	10.2	10.6	12.8	9.2
3	18.3	19.6	10.2	17.7	19.2	10.8	13.6	14.5	8.8

highlighting the improved power efficiency characteristics that are achieved for the hybrid design with increased mobility. This is to be expected given that AW inherently seeks to decrease the magnitude of the controller output.

It is also worth noting that the vast majority of the complexity of the proposed hybrid solution lies in the synthesis routine, therefore very little additional computational overhead was experienced during practical implementation. Empirical evidence suggests little or no difference between the AW approach and a more conventional adaptive step size power control approach in terms of microcontroller activity during realtime experiments. The attendant performance improvements are even more pronounced when 802.15.4 based mote devices with enhanced computational capabilities, like e.g. the Intel Shimmer hardware platform [23], are considered.

6. CONCLUDING REMARKS

This paper has presented a new strategy for power control in wireless sensor networks where operational longevity is an issue. An a priori level of performance is achieved in terms of packet error rate using minimum power where significant quantisation noise exists in the selection of

the appropriate transmission power. Robustness to a variety of communication constraints have

been illustrated using an anti-windup scheme. The new approach provides a methodology for

the rigorous assessment of the effect that a general class of static memory-less nonlinearity can

have on overall system performance. Future work will consider the dynamic management of

floor levels on the carrier sense threshold, hopefully leading to further significant power savings

in this setting

7. APPENDICES

7.1. Static Minimal Realizations

Given the state space realization of the plant

$$
\begin{bmatrix} G_1 & G_2 \end{bmatrix} \sim
\left[
\begin{array}{c|c}
A_p & B_{pd}B_p \\
\hline
C_p & D_{pd}D_p
\end{array}
\right]
$$

then the minimal realization is given by

$$
\bar{x} = \begin{bmatrix} x_p \\ x_c \end{bmatrix},
\bar{A} = \begin{bmatrix} A_p + B_p\tilde{\Delta}D_cC_p & B_p\tilde{\Delta}C_c \\ B_c\Delta C_p & A_c + B_c\Delta D_pC_c \end{bmatrix}
$$

$$
B_0 = \begin{bmatrix} B_p\tilde{\Delta} \\ B_c\Delta D_p \end{bmatrix},
\bar{B} = \begin{bmatrix} B_p\tilde{\Delta} & -B_p\tilde{\Delta}D_c \\ B_c\Delta D_p & -B_c\Delta \end{bmatrix}
$$

$$
\bar{C}_1 = \begin{bmatrix} \tilde{\Delta}D_cC_p & \tilde{\Delta}C_c \end{bmatrix},
D_{01} = \tilde{\Delta}D_cD_p,
\bar{D}_1 = \begin{bmatrix} I + \tilde{\Delta}D_cD_p & -\tilde{\Delta}D_c \end{bmatrix}
$$

$$
\bar{C}_2 = \begin{bmatrix} \Delta C_p & \Delta D_pC_c \end{bmatrix},
D_{02} = \Delta D_p,
\bar{D}_2 = \begin{bmatrix} \Delta D_p & -\Delta D_pD_c \end{bmatrix}
$$

REFERENCES

1. R. Szewczyk D. Culler A. Mainwaring, J. Polastre and J. Anderson, Wireless sensor networks for habitat monitoring, *In Proceedings of the 1st ACM international workshop on Wireless sensor networks and applications* 2002, pp. 88-97.

2. Tia Gao, Christopher Pesto, Leo Selavo, Yin Chen, JeongGil Ko, JongHyun Lim, Andreas Terzis, Andrew Watt, James Jeng, Bor-rong Chen, Konrad Lorincz, and Matt Welsh, Wireless Medical Sensor Networks in Emergency Response: Implementation and Pilot Results, *In Proceedings of the 2008 IEEE International Conference on Technologies for Homeland Security*, Waltham, MA, May 2008.

3. B. Zurita Ares, C. Fischione, A. Speranzon, and K. H. Johansson. On power control for wireless sensor networks: system model, middleware component and experimental evaluation. *European Control Conference*, Kos, Greece, 2007.

4. M. Walsh, M. Hayes, and J. Nelson, Robust Performance for an Energy Sensitive Wireless Body Area Network - An Anti-Windup Approach,*International Journal of Control*, Accepted for publication, 2008.

5. K. Srinivasan and P. Levis, RSSI is Under Appreciated, *Third Workshop on Embedded Networked Sensors (EmNets)*, 2006

6. S. A. Grandhi, J. Zander, and R. Yates, Constrained power control, *Wireless Personal Communications*, 1995, (2)(3).

7. M. Andersin, Z. Rosberg, and J. Zander, Distributed discrete power control in cellilar pcs, *Wireless Personal Communications*, 1998, (3)(6).

8. M. Turner, G. Herrmann and I. Postlethwaite, Incorporating robustness requirements into anti-windup design, *IEEE Transactions on Automatic Control*, 2007, (52)(10): 1842-1855.

9. D.S. Bernstein and A.N. Michel, A chronological bibliography on saturating actuators, *International Journal of Robust and Nonlinear Control*, 1995, (5): 375-380.

10. P.F. Weston and I. Postlewaite, Analysis and design of linear conditioning schemes for systems containing saturating actuators, *Automatica*, 36(9), 2000.

11. G. Herrmann, M. Turner and I. Postlethwaite, Discrete-time and sampled-data anti-windup synthesis: stability and performance, *International Journal of Systems Science*, 2006, (37)(2): 91-114.

12. F. Gunnarsson, F. Gustafsson, and J. Blom, Pole placement design of power control algorithms, *In Proc. IEEE Vehicular Technology Conference*, Houston, TX, USA, May 1999.

13. IEEE Computer Society, Wireless lan medium access control (mac) and physical layer (phy) specifications for low-rate wireless personal area networks (lr-wpans), IEEE Std 802.15.4 (2006).

14. A. Goldsmith, *Wireless Communications*, Cambridge University Press; 2006.

15. I. Horowitz, Survey of quantitative feedback theory (QFT), *Int. J. Robust Nonlinear Control*, Vol. 11, 2001, pp. 887–921.

16. C. Borghesani, Y. Chait, and O. Yaniv, *The QFT Frequency Domain Control Design Toolbox For Use with MATLAB*, Terasoft, Inc., 2003.

17. R. Hanus, M. Kinnaert and J. Henrotte, Conditioning technique a general anti-windup and bumpless transfer method, *Automatica*, 1987, (23): 729-39.

18. M. Turner and I. Postlethwaite, A new perspective on static and low-order anti-windup synthesis, *International Journal of Control*, 2004, (77): 27-44.

19. G. Herrmann, M.C. Turner, I. Postlethwaite and G. Guo, Practical Implementation of a Novel Anti-Windup Scheme in a HDD-Dual-Stage Servo-System, *IEEE/ASME Transactions on Mechatronics*, 2004, (9)(3).

20. A.R. Teel and N. Kapoor, The L2 anti-windup problem: Its definition and solution, *in Proc. Eur. Control Conf*, 1997.

21. MIABOT Pro fully autonomous miniature mobile robot.
    http://www.merlinrobotics.co.uk/merlinrobotics/, [November 10, 2008]

22. Yuan-Ho Chen Bore-Kuen Lee and Bor-Sen Chen, Robust Hinf Power Control for CDMA Cellular Communication Systems, *IEEE Transactions on Signal Processing*, 2006, (54)(10): 3947–3956.

23. Shimmer Hardware PLatform.
    http://shimmer-research.com/, [December 3, 2008]